Proceedings of the 11th International Conference on Environmental Remediation and Radioactive Waste Management
ICEM2007
September 2-6, 2007, Oud Sint-Jan Hospital Conference Center, Bruges, Belgium

ICEM07-7109

ON THE ROLE OF H_2 AS AN INHIBITOR OF UO_2 MATRIX DISSOLUTION

Juan Merino / ENVIROS **Xavier Gaona / ENVIROS**

Lara Duro / ENVIROS **Jordi Bruno / ENVIROS** **Aurora Martínez-Esparza / ENRESA**

ABSTRACT

The study of spent fuel behaviour under disposal conditions is usually based on conservative approaches assuming oxidising conditions produced by water radiolysis at the fuel/water interface. However, the presence of H_2 from container corrosion can inhibit the dissolution of the UO_2 matrix and enhance its long-term stability. Several studies have confirmed the decrease in dissolution rates when H_2 is present in the system, although the exact mechanisms of interaction have not been fully established. This paper deals with a radiolytic modelling exercise to explore the consequences of the interaction of H_2 with radicals generated by radiolysis in the homogeneous phase. The main conclusion is that in all the modelled cases the presence of H_2 in the system leads to a decrease in matrix dissolution. The extent of the inhibition, and the threshold partial pressure for the inhibition to take place, both depend in a complex way on the chemical composition of the water and the type of radiation present in the system

INTRODUCTION

Direct disposal of spent nuclear fuel, without reprocessing, is the option chosen by many countries, including Spain, for the final disposal of this type of waste. The Spanish concept of direct disposal consists of a waste package inside a steel canister, surrounded by bentonite in a deep tunnel excavated in granitic or clay host rock. The most credible mechanism whereby radionuclides present in the spent fuel can reach the biosphere is water mediated transport. Intrusion of water into the spent fuel canister can be due to an early canister failure or long term corrosion at the end of the canister lifetime. Therefore much effort has been devoted to study spent fuel dissolution under different conditions in the last decades. When evaluating spent fuel behaviour under disposal conditions, pessimistic or conservative approaches are usually followed, assuming oxidising conditions in the local near field due to radiolytic oxidants generated by water radiolysis at the fuel/water interface.

However, the presence of H_2 arising from radiolysis or, more importantly, container and cladding corrosion, has been shown to clearly inhibit the dissolution of the UO_2 matrix, enhancing its long-term stability. For example, Röllin et al. (2001) carried out flow-through dissolution experiments with spent fuel under 1 atm of H_2. They observed a decrease in the matrix dissolution rate of more than 3 orders of magnitude with respect to oxidising conditions. Spahiu and co-workers measured very low concentrations of radionuclides in spent fuel dissolution tests under high H_2 pressures (Spahiu et al., 2002, 2004). Experiments with alpha-doped UO_2 pellets in the presence of H_2 (Carbol et al., 2005) showed again very low dissolution rates. The main conclusion of this study and other supporting evidence was that above a certain H_2 concentration (so called threshold concentration) the production of radiolytic oxidants is extremely small, being very difficult to quantify experimental dissolution rates. The H_2 threshold concentration depends on many factors, among them the type and intensity of radiation and the chemical composition or the water.

Electrochemical studies have also shown the effect of H_2 on suppressing the UO_2 corrosion potential (King and Shoesmith, 2004). Dissolved hydrogen can polarize the UO_2 surface to reducing potentials as a consequence of H_2 activation (Broczkowski et al. 2005). These last authors even showed that ε particles present in the SIMFUEL surface could have a galvanic coupling between those particles and the UO_2 matrix leading to the suppression of the corrosion potential. Other studies have focused on the reactivity of H_2 towards the uranyl ion, UO_2^{2+} (Ekeroth et al., 2004). They found that the reduction to UO_2 could proceed without a catalyzer provided that pressures and temperatures are sufficiently high.

From all the supporting evidence, several mechanisms have been proposed to explain how H_2 can interact with the system and inhibit UO_2 dissolution:

- Reaction of H_2 in homogeneous medium with radiolytic OH radical
- Catalytic decomposition of H_2 (activation of H_2 in atomic hydrogen) in the UO_2 surface or in the ε particles.
- Reduction of oxidized uranium in the surface
- Reduction of oxidized uranium in solution (it depends on water speciation).

In this paper a radiolytic modelling exercise has been carried out to explore the consequences of the first mechanism involving the reaction of H_2 with radicals generated by radiolysis in the homogeneous phase.

CONCEPTUAL MODEL

A hypothetical system consisting of a closed batch reactor with a solid, a liquid phase and a gas phase has been selected (see Figure 1). The solid is unirradiated UO_2 and the liquid phase contains deionized water. The gas phase is considered to be an inert gas under atmospheric pressure mixed with varying concentrations of H_2. The liquid phase is homogeneously irradiated with either alpha or beta radiation.

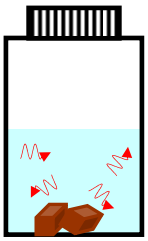

Figure 1. System considered for the radiolytic modelling

The parameters considered in this hypothetical system were:

- Aqueous phase and gas phase, $V_{aq} = V_{gas} = 2.4$ ml.
- Deionized water.
- Homogeneous radiation field (either α or β/γ) with a constant dose rate of 14.2 $mGy \cdot s^{-1}$.
- G-values taken from Christensen, 1998 (see Table I)
- Radical recombination scheme (see Table II) taken from Pastina and Laverne 2001 and the Notre Dame Radiation Laboratory on-line database http://www.rcdc.nd.edu/index.html
- Equilibrium reactions for the gaseous species (H_2, O_2) following Henry's law (see Table III).

Table I. G-values used in the calculations

	G (molec/100eV)	
Species	**A radiation**	**β/γ radiation**
OH	0.24	2.67
e_{aq}^-	0.06	2.66
H	0.21	0.55
H_2	1.3	0.45
H_2O_2	0.985	0.72
H^+	0.06	2.76
OH^-		0.1
HO_2	0.22	
H_2O	-2.71	-6.87

Table II. Reactions and rate constants for the radical recombination scheme in deionized water (from

Reactions	**Kinetic constant ($M^{-1} \cdot s^{-1}$ o s^{-1})**
Acid-base reactions	
$H^+ + OH^- \rightarrow H_2O$	$1.42 \cdot 10^{11}$
$H_2O \rightarrow H^+ + OH^-$	$2.57 \cdot 10^{-5}$
$H_2O_2 \rightarrow H^+ + HO_2^-$	$6.31 \cdot 10^{-2}$
$H^+ + HO_2^- \rightarrow H_2O_2$	$3.50 \cdot 10^{10}$
$OH^- + H_2O_2 \rightarrow HO_2^- + H_2O$	$1.14 \cdot 10^{9}$
$HO_2^- + H_2O \rightarrow OH^- + H_2O_2$	$1.02 \cdot 10^{4}$
$e_{aq}^- \rightarrow H + OH^-$	$1.80 \cdot 10^{1}$
$OH^- + H \rightarrow e_{aq}^-$	$2.00 \cdot 10^{7}$
$H + H_2O \rightarrow e_{aq}^- + H^+$	3.91
$H^+ + e_{aq}^- \rightarrow H + H_2O$	$4.06 \cdot 10^{10}$
$OH + OH^- \rightarrow O^- + H_2O$	$1.25 \cdot 10^{10}$
$O^- + H_2O \rightarrow OH + OH^-$	$1.26 \cdot 10^{7}$
$OH \rightarrow O^- + H^+$	$1.26 \cdot 10^{-1}$
$O^- + H^+ \rightarrow OH$	$1.00 \cdot 10^{11}$
$HO_2 \rightarrow H^+ + O_2^-$	$1.08 \cdot 10^{6}$
$O_2^- + H^+ \rightarrow HO_2$	$5.50 \cdot 10^{10}$
$HO_2 + OH^- \rightarrow O_2^- + H_2O$	$5.00 \cdot 10^{10}$
$O_2^- + H_2O \rightarrow HO_2 + OH^-$	$1.03 \cdot 10^{3}$
Chemical reactions	
$e_{aq}^- + OH \rightarrow OH^- + H_2O$	$5.00 \cdot 10^{10}$
$e_{aq}^- + H \rightarrow H_2 + OH^-$	$2.90 \cdot 10^{10}$
$e_{aq}^- + H_2O_2 \rightarrow OH^- + OH + H_2O$	$1.13 \cdot 10^{10}$
$e_{aq}^- + HO_2 \rightarrow HO_2^- + H_2O$	$2.00 \cdot 10^{10}$
$e_{aq}^- + O_2^- \rightarrow HO_2^- + OH^-$	$1.30 \cdot 10^{10}$
$e_{aq}^- + O_2 \rightarrow O_2^- + H_2O$	$2.00 \cdot 10^{10}$
$e_{aq}^- + O^- \rightarrow OH^- + OH^-$	$2.20 \cdot 10^{10}$
$e_{aq}^- + HO_2^- \rightarrow O^- + OH^- + H_2O$	$3.50 \cdot 10^{9}$
$e_{aq}^- + e_{aq}^- \rightarrow H_2 + OH^- + OH^-$	$6.00 \cdot 10^{9}$
$e_{aq}^- + O_3 \rightarrow O_3^- + H_2O$	$3.60 \cdot 10^{10}$
$e_{aq}^- + O_3^- \rightarrow O_2 + OH^- + OH^-$	$1.60 \cdot 10^{10}$
$H + OH \rightarrow H_2O$	$1.35 \cdot 10^{10}$
$H + H \rightarrow H_2$	$8.50 \cdot 10^{9}$
$H + H_2O_2 \rightarrow OH + H_2O$	$6.30 \cdot 10^{7}$
$H + HO_2 \rightarrow H_2O_2$	$1.90 \cdot 10^{10}$

Reactions	Kinetic constant ($M^{-1}\cdot s^{-1}$ o s^{-1})
$H + O_2^- \rightarrow HO_2^-$	$1.90\cdot10^{10}$
$H + O_2 \rightarrow HO_2$	$1.55\cdot10^{10}$
$H + O^- \rightarrow OH^-$	$1.00\cdot10^{10}$
$H + HO_2^- \rightarrow OH^- + OH$	$3.29\cdot10^{8}$
$H + O_3^- \rightarrow OH^- + O_2$	$1.00\cdot10^{10}$
$H + O_3 \rightarrow OH + O_2$	$2.20\cdot10^{10}$
$OH + OH \rightarrow H_2O_2$	$4.90\cdot10^{9}$
$OH + H_2 \rightarrow H + H_2O$	$4.70\cdot10^{7}$
$OH + H_2O_2 \rightarrow HO_2 + H_2O$	$3.85\cdot10^{7}$
$OH + HO_2 \rightarrow H_2O + O_2$	$9.00\cdot10^{9}$
$OH + O_2^- \rightarrow OH^- + O_2$	$9.50\cdot10^{9}$
$OH + O^- \rightarrow HO_2^-$	$5.00\cdot10^{9}$
$OH + HO_2^- \rightarrow O_2^- + H_2O$	$6.95\cdot10^{9}$
$OH + HO_2^- \rightarrow OH^- + HO_2$	$6.25\cdot10^{9}$
$OH + O_3 \rightarrow HO_2 + O_2$	$1.05\cdot10^{8}$
$OH + O_3^- \rightarrow O_2^- + HO_2$	$8.50\cdot10^{9}$
$OH + O_3^- \rightarrow O_3 + OH^-$	$2.60\cdot10^{9}$
$OH + O_3^- \rightarrow O_2^- + O_2^- + H^+$	$6.00\cdot10^{9}$
$HO_2 + H_2O_2 \rightarrow OH + H_2O + O_2$	$1.73\cdot10^{-1}$
$HO_2 + HO_2 \rightarrow H_2O_2 + O_2$	$5.31\cdot10^{6}$
$HO_2 + O_2^- \rightarrow HO_2^- + O_2$	$5.55\cdot10^{7}$
$HO_2 + O^- \rightarrow O_2 + OH^-$	$6.00\cdot10^{9}$
$HO_2 + H_2O_2 \rightarrow OH + H_2O + O_2$	2.4
$HO_2 + HO_2^- \rightarrow OH + O_2 + OH^-$	$5.00\cdot10^{-1}$
$HO_2 + O_3 \rightarrow HO_3 + O_2$	$5.00\cdot10^{8}$
$HO_2 + O_3^- \rightarrow O_2 + O_2 + OH^-$	$6.00\cdot10^{9}$
$O_2^- + H_2O_2 \rightarrow OH^- + OH + O_2$	$5.47\cdot10^{-1}$
$O_2^- + HO_2^- \rightarrow O^- + O_2 + OH^-$	$1.30\cdot10^{-1}$
$O^- + O_2 \rightarrow O_3^-$	$3.25\cdot10^{9}$
$O_3^- \rightarrow O^- + O_2$	$4.40\cdot10^{3}$
$O^- + H_2 \rightarrow e_{aq}^-$	$9.50\cdot10^{7}$
$O^- + H_2 \rightarrow H + OH^-$	$8.00\cdot10^{7}$
$O^- + H_2O_2 \rightarrow O_2^- + H_2O$	$5.00\cdot10^{8}$
$O^- + HO_2^- \rightarrow O_2^- + OH^-$	$4.00\cdot10^{8}$
$O^- + O_3 \rightarrow O_2^- + O_2$	$5.00\cdot10^{9}$
$O^- + O_3^- \rightarrow O_2^- + O_2^-$	$7.00\cdot10^{8}$
$O + H_2O_2 \rightarrow OH + HO_2$	$1.60\cdot10^{9}$
$O + O_2 \rightarrow O_3$	$4.00\cdot10^{9}$
$O_3 \rightarrow O + O_2$	$3.00\cdot10^{-6}$
$O + OH^- \rightarrow HO_2^-$	$4.20\cdot10^{8}$
$O + HO_2^- \rightarrow OH + O_2^-$	$5.30\cdot10^{9}$
$O_3 + H_2O_2 \rightarrow HO_2 + OH + O_2$	$2.06\cdot10^{-2}$
$O_3 + O_2^- \rightarrow O_3^- + O_2$	$1.55\cdot10^{9}$
$O_3 + OH^- \rightarrow HO_2^- + O_2$	55
$O_3 + HO_2^- \rightarrow O_2^- + OH + O_2$	$5.50\cdot10^{6}$
$O_3^- + H^+ \rightarrow OH + O_2$	$9.00\cdot10^{10}$
$HO_3 \rightarrow O_2 + OH$	$1.10\cdot10^{5}$

Table III. Reactions and rate constants for the gas-aqueous phase equilibria derived from Henry's law.

Reactions	Kinetic constant (s^{-1})
$O_2 \rightarrow O_2(g)$	$3.25\cdot10^{3}$
$H_2 \rightarrow H_2(g)$	$5.04\cdot10^{3}$
$O_2(g) \rightarrow O_2$	100
$H_2(g) \rightarrow H_2$	100

The parameters related to the solid phase are the following:

- Mass of UO_2: 0.02 g
- Reactive surface: 24 cm^2
- Density of sites: $2.74\cdot10^{-6}$ $mol\cdot dm^{-2}$
- Mechanism of oxidative dissolution of UO_2, see Table IV (a revised version of the mechanism developed in Martinez-Esparza et al., 2005).

Table IV. Mechanism of oxidative dissolution of UO_2. The symbol ">" shows a surface species converted to an equivalent concentration by means of the solid to volume ratio.

Reactions	Kinetic constants ($M^{-1}\cdot s^{-1}$)
Oxidation mechanism	
$>UO_2 + H_2O_2 \rightarrow >UO_2 + OH + OH$	2.2
$>UO_2 + OH \rightarrow >UO_2OH$	$2.6\cdot10^{4}$
$>UO_2OH + OH \rightarrow >UO_3 + H_2O$	$1\cdot10^{15}$
$>UO_2 + O_2 \rightarrow >UO_2\text{-}O_2$	$2.1\cdot10^{-3}$
$>UO_2\text{-}O_2 + >UO_2 \rightarrow >UO_3 + >UO_3$	$1\cdot10^{16}$
Dissolution mechanism	
$>UO_3 + H^+ \rightarrow UO_2(OH)^+$	0.018
$>UO_3 + H_2O \rightarrow UO_2(OH)_2$	$6.6\cdot10^{-10}$
$>UO_3 + HO_2^- \rightarrow UO_3HO_2^-$	75
$>UO_3 + HO_2 \rightarrow UO_3HO_2$	200

The kinetic code CHEMSIMUL (Kirkegaard and Bjergbakke, 2002) has been used to simulate the evolution of the chemical system under the different conditions under study. Simulations have been carried out in a standard PC, requiring less than a second of CPU time.

SIMULATIONS WITH NO SOLID (HOMOGENEOUS RADIOLYSIS)

In order to test the intrinsic evolution of the homogenous phase in the absence of the solid, a series of simulations have been carried out without the UO_2 which are described in this section.

The first series of simulations involved several initial H_2 partial pressures in a β/γ radiation field (Figure 2). As was already described by Pastina and LaVerne (2001), the presence

of an initial H_2 concentration in the system significantly inhibits the generation of oxidizing species (H_2O_2 and O_2).

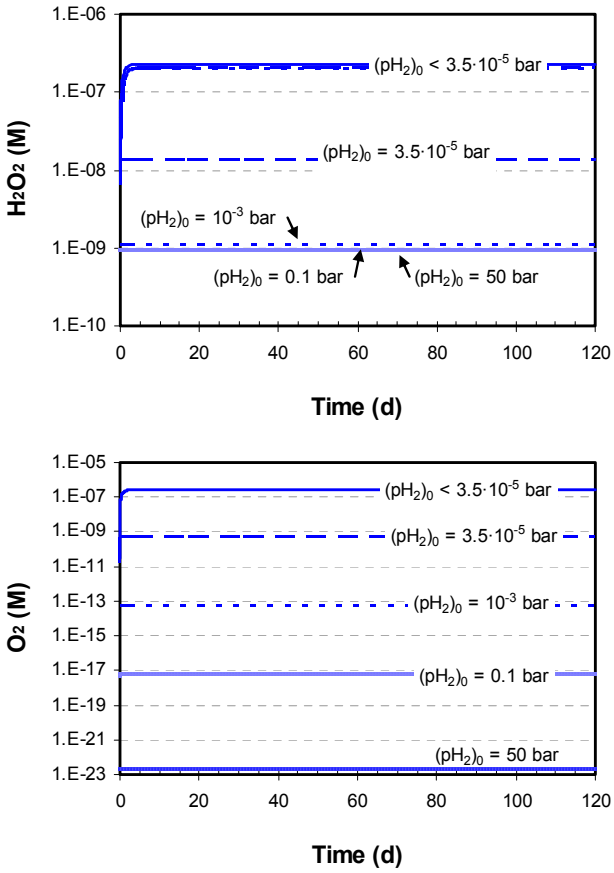

Figure 2. Evolution of the main radiolysis species under different initial H_2 partial pressures in a β/γ radiation field in the absence of solid.

This effect can be explained through the radical recombination mechanism, where H_2 reacts with OH giving place to the formation of the radical H, which is the main consumer of molecular species. This inhibition only takes place when the initial partial pressure of H_2 is greater than $3.5 \cdot 10^{-5}$ bar, which can be thought of as a threshold concentration. Below this initial concentration, the system evolves as if there were no H_2 at all, leading to a steady state.

The same set of simulations with α radiation instead of β/γ radiation is shown in Figure 3. As was the case for β/γ radiation, the model also predicts an inhibition effect caused by the presence of H_2. In the case of α radiation, however, the threshold partial pressure is significantly higher, $1.5\ 10^{-3}$ bar. This is not unexpected as alpha radiation, being of higher LET, has a bigger capacity of generating molecular products.

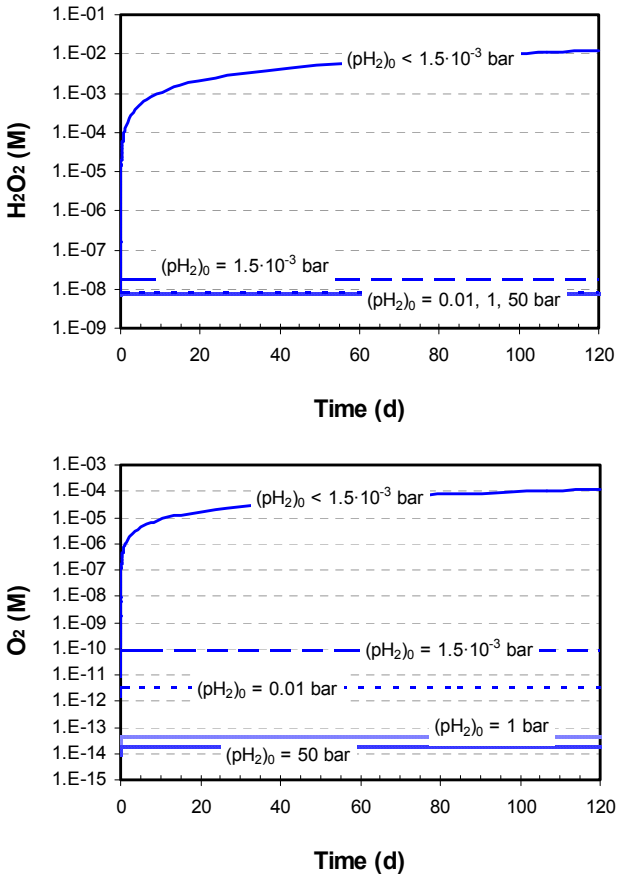

Figure 3. Evolution of the main radiolysis species under different initial H_2 partial pressures in a α radiation field in the absence of solid.

However, this model prediction is at odds with experimental evidence where virtually no effect on H_2O_2 formation is found in H_2 saturated solutions irradiated with 5 MeV helium ions (Pastina and LaVerne, 2001). These authors also report a discrepancy between the radiolytic model and the experimental data. The lack of validity of the homogeneous model under high LET radiation was raised by the authors as the likely explanation for this discrepancy. Another possibility, already mentioned in the referenced work, is the role of the impurities present in the system. To explore this possibility, we have carried out a new set of simulations where we have introduced a trace amount of O_2 in the system (1 mbar of O_2, representing a plausible intrusion of air in the system). The result of this simulation is given in Figure 4, where it is clearly seen that, under the presence of trace amounts of O_2, the threshold H_2 partial pressure that the model predicts (2.8 bar) is orders of magnitude higher than in the absence of O_2. In other words, the inhibition effect of H_2 is only seen under very high pressures, which would be in agreement with the available experimental evidence. The reason why the presence of O_2 affects the behaviour of the system must be found in the chain reaction, where it acts as a supplier of OH radicals under high LET radiation and therefore a higher concentration of H_2 is needed to scavenge them.

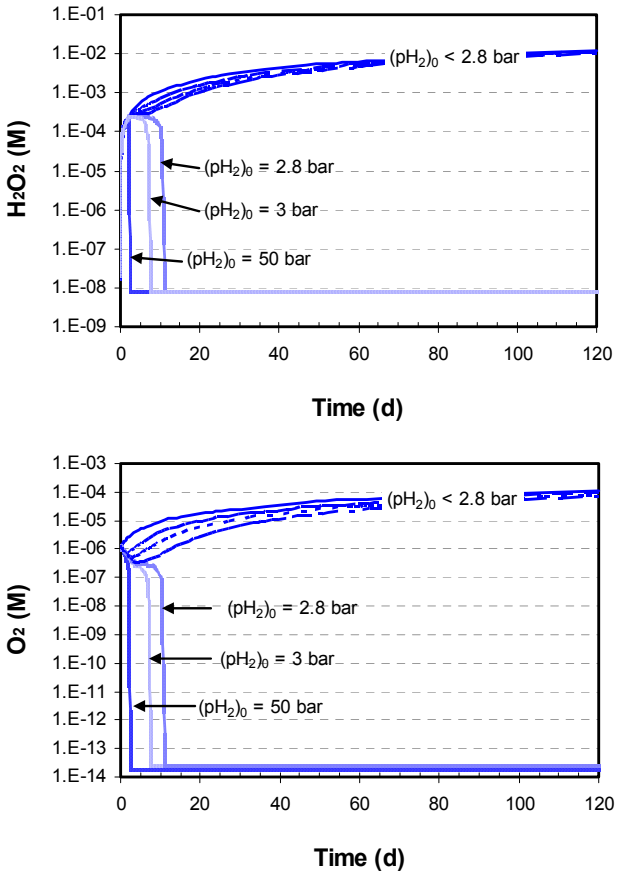

Figure 4. Evolution of the main radiolysis species under different initial H_2 partial pressures in a α radiation field in the absence of solid with an initial trace of O_2.

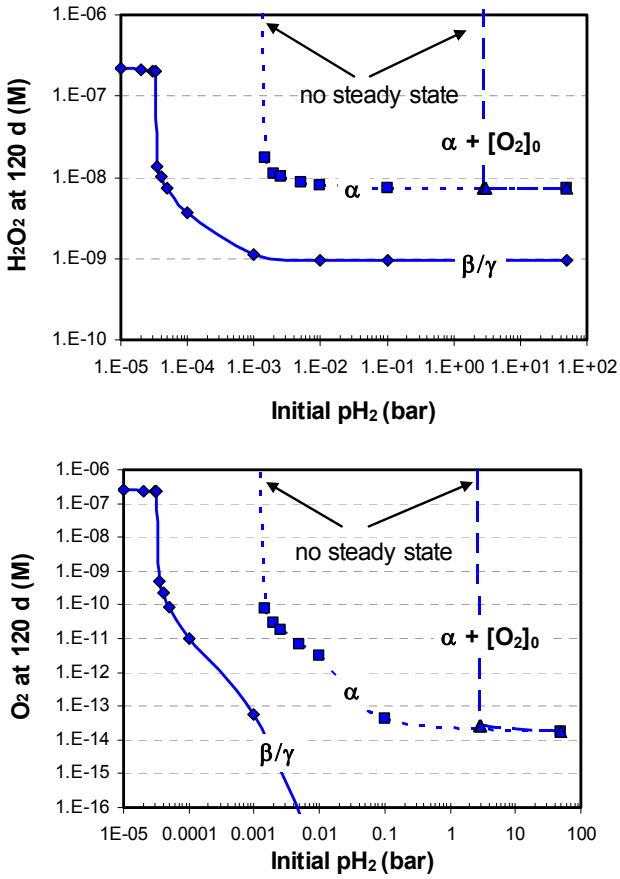

Figure 5. Steady state concentrations (simulation time 120 d) of H_2O_2 and O_2 for the different studied cases.

The same simulations with an oxygen impurity in a β/γ radiation field (not shown) leads to a threshold pressure of only one order of magnitude higher that in the absence of O_2. That is, O_2 has less influence on the inhibition effect of H_2 under gamma radiation that under alpha radiation. This must be related to the low LET of gamma radiation and its interaction with the O_2 present in the system which would not be able to scavenge OH radicals at same rate as with alpha radiation. Figure 5 shows a comparison of the achieved concentrations in the steady state for all initial H_2 partial pressures. The threshold H_2 concentration is clearly seen in all the cases studied.

SIMULATIONS WITH UO_2

The next series of runs were done introducing the solid into the system. It is assumed that the interaction of H_2 only occurs in the homogenous phase, that is, no activation of H_2 is produced at the surface. Two sets of simulations have been carried out, one for a β/γ radiation field and another one for an α radiation field. The evolution of concentrations of the molecular radiolysis products under β/γ radiation is shown in Figure 6. The result of the simulation with no solid at initial $pH_2 = 0$ is also given for comparison purposes. As it can be seen from the graph, the introduction of the solid dramatically changes the evolution of the radiolytic system. This is due to the fact that the oxidation-dissolution mechanism of UO_2 involves the decomposition of H_2O_2 in OH radicals. H_2O_2 concentrations decrease to approximately the same levels irrespective of the initial H_2 partial pressure, as it is somehow "buffered" by the surface and recombination of radicals. Oxygen, on the other hand, is depleted to very low levels even in the absence of an initial H_2 partial pressure as a result of its consumption at the surface coupled to the inhibition effect of H_2.

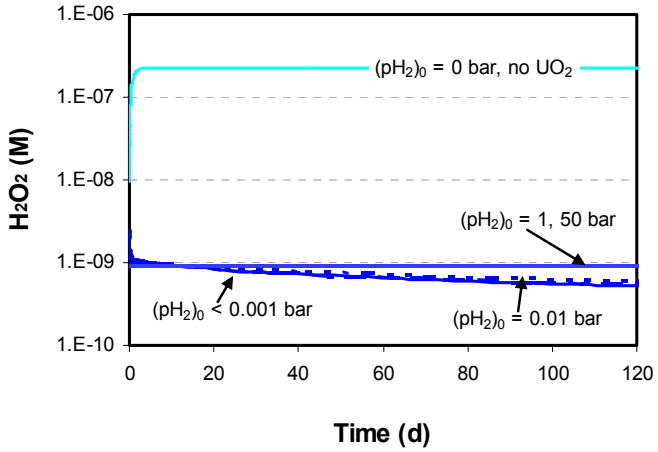

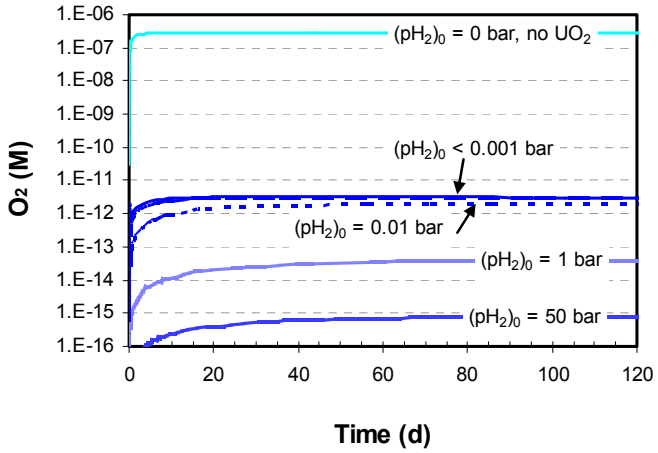

Figure 6. Evolution of the main radiolysis species under different initial H_2 partial pressures in a β/γ radiation field when solid UO_2 is present in the system.

The amounts of dissolved moles of uranium, together with its time derivative converted to dissolution rate are shown in Figure 7. For all initial H_2 partial pressure the pattern is similar, an initial increase in the dissolution rate until a steady state is reached. The dissolution rate at the steady state strongly depends on the initial H_2 partial pressure. It could also be said that the threshold H_2 pressure is approximately 0.001 bar.

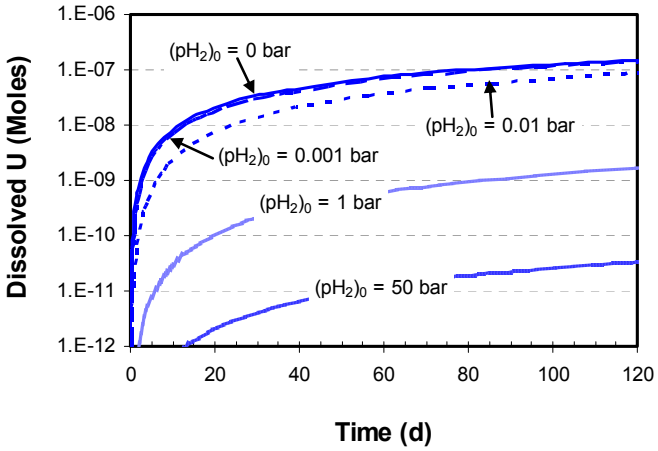

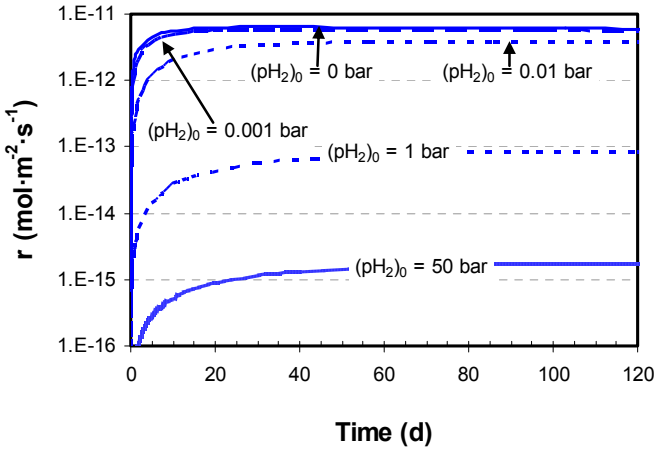

Figure 7. Evolution of moles of uranium dissolved and its corresponding dissolution rate under different initial H_2 partial pressures in a β/γ radiation field when solid UO_2 is present in the system.

The last series of simulations involved the presence of an α radiation field. The evolution of the main molecular products is shown in Figure 8. As was the case for β/γ radiation, the presence of the solid has a strong influence in the evolution of the oxidants. Even when there is not an initial H_2 partial pressure, oxidants do not accumulate in the system, as the surface acts as an oxidant consumer leading to a kinetic balance. It is interesting to note the sharp decrease in oxidants concentrations after several days of simulation time for initial partial pressures up to 0.003 bar. There is not a clear explanation for this, but it may be related to a transitory effect caused by the highly coupled, second order differential equations representing the chemical system.

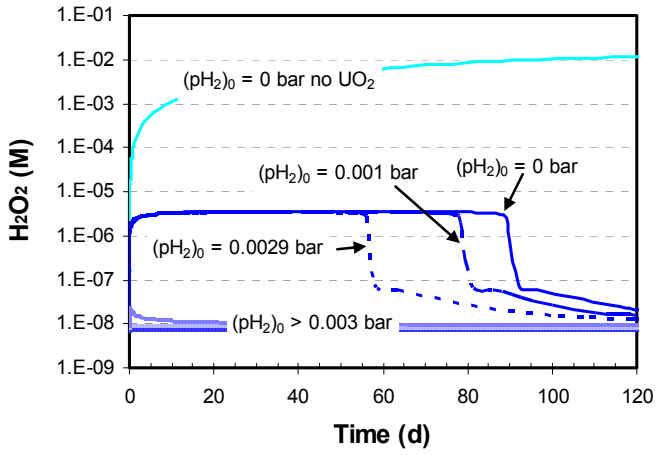

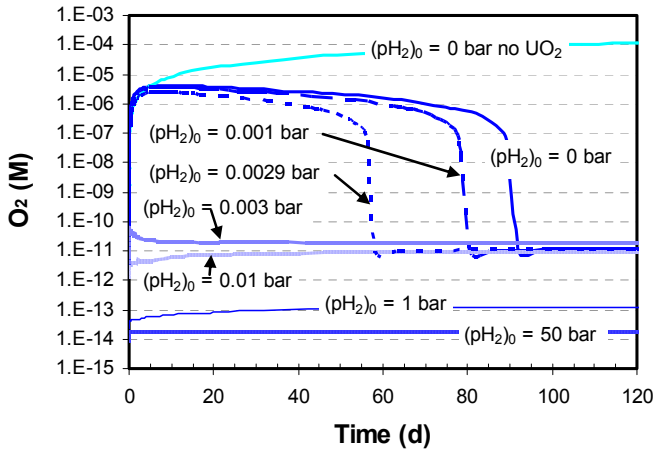

Figure 8. Evolution of the main radiolysis species under different initial H_2 partial pressures in a α radiation field when solid UO_2 is present in the system.

Regarding moles of dissolved uranium and corresponding dissolution rates, their evolution with time is shown in Figure 9. The effect of increasing the initial H_2 partial pressure is clearly seen in this graph. Due to the fact that the system shows a relatively long transitory state, the threshold initial H_2 partial pressure depends on the time of evaluation. At 20 days of simulation time the threshold pressure is approximately 0.003 bar, whereas at 120 days of evaluation time the threshold pressure increases up to 0.01 bar..

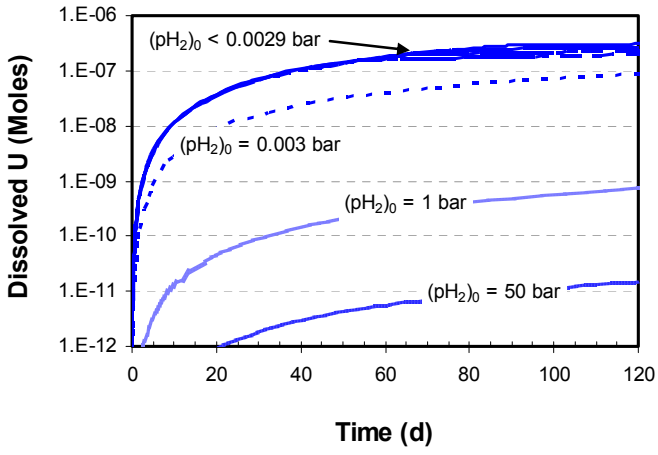

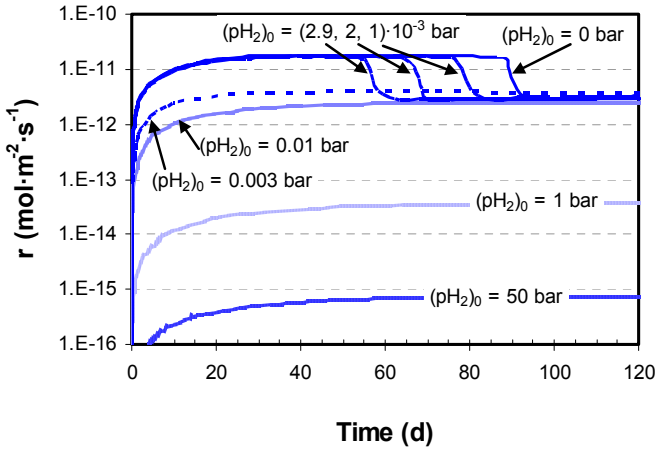

Figure 9. Evolution of moles of uranium dissolved and its corresponding dissolution rate under different initial H_2 partial pressures in a α radiation field when solid UO_2 is present in the system.

As a summary of the main findings, we have plotted in Figure 10 the dissolution rates as a function of the initial H_2 partial pressure for the hypothetical system studied here for both β/γ and α radiation. In the case of β/γ radiation the dissolution rates correspond to the steady state at 120 days of simulation, whereas in the case of α radiation we have been forced to choose two simulation times, 20 and 120 days, to take into account the relatively long transitory state. From this graph it is clear that H_2 has an inhibition effect on UO_2 dissolution and that this effect is a threshold phenomenon.

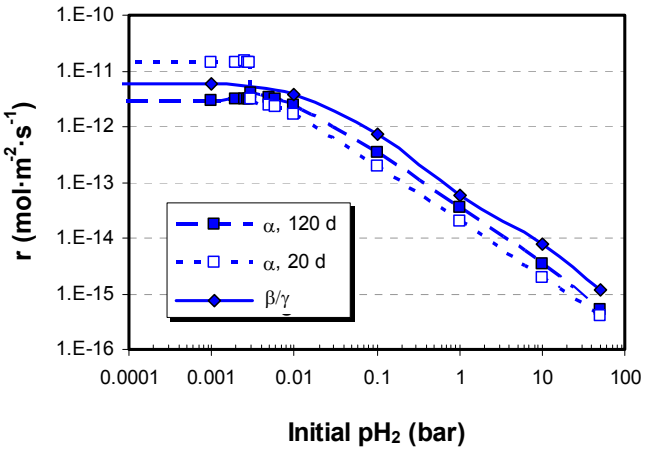

Figure 10. Dissolution rate as a function of the initial H_2 partial pressure in the hypothetical system studied in this work.

It must be highlighted that the model only takes into account the interaction of H_2 with radicals in the homogenous phase. Thus, the modelling exercise carried out in this work suggests that this process is able to explain, at least partially, the inhibition effect of H_2 on the dissolution of spent fuel. As a final remark, it should be remember that the numerical results given here are only valid for the hypothetical system under study. Under other conditions (water composition, irradiated volume, geometry, ..) the threshold pressures would certainly change.

CONCLUSIONS

The results show that in all cases the presence of H_2 in the system leads to a decrease in matrix dissolution. The extent of the inhibition, and the threshold partial pressure for the inhibition to take place, both depend in a complex way on the chemical composition of the water and the type of radiation present in the system.

ACKNOWLEDGMENTS

This work has been financially supported by ENRESA.

REFERENCES

Broczkowski M.E., Noël J.J. and Shoesmith D.W. (2005). Electrochemical, SECM, and XPS studies of the influence of H_2 on UO_2 nuclear fuel corrosion. In: MRS 2005, 29th International Symposium on the Scientific Basis for Nuclear Waste Management. Ghent, Belgium, 12-16 September 2005.

P. Carbol, J. Cobos-Sabate, J.-P. Glatz, C. Ronchi, V. Rondinella, D. H. Wegen, T. Wiss, A. Loida, V. Metz, B. Kienzler, K. Spahiu, B. Grambow, J. Quiñones and A. Martinez- Esparza Valiente, (2005). The effect of dissolved hydrogen on the dissolution of ^{233}U doped UO_2(s), high burn-up spent fuel and MOX fuel. SKB Technical Report TR-05-09.

H. Christensen, 1998. Calculations simulating spent-fuel leaching experiments. Nuclear Technology, vol. 124, 165-174.

Ekeroth E., Jonsson M., Eriksen T.E., Ljungqvist K., Kovács S. and Puigdomènech I. (2004). Reduction of UO_2^{2+} by H_2. J. Nucl. Mater. 334, pp. 35-39.

King F. and Shoesmith D. (2004). Electrochemical studies of the effect of H_2 on UO_2 dissolution. SKB Technical Report TR-04-20.

P. Kirkegaard and E. Bjergbakke, 2002. CHEMSIMUL: A simulator for chemical kinetics. Risø–R–1085(EN). http://www.risoe.dk/ita/chemsimul.

A. Martínez-Esparza, M.A. Cuñado, J.A. Gago, J. Quiñones, E. Iglesias, J. Cobos, A. González de la Huebra, E. Cera, J. Merino, J. Bruno, J. de Pablo, I. Casas, F. Clarens, J. Giménez, 2005. Development of a Matrix Alteration Model (MAM). Publicación Técnica Enresa 01/2005.

B. Pastina and J. LaVerne, 2001. Effect of Molecular Hydrogen on Hydrogen Peroxide in Water Radiolysis, J. Phys. Chem. A, 105, 9316-9322.

Röllin S., Spahiu K. and Eklund U.-B., 2001. Determination of dissolution rates of spent fuel in carbonate solutions under different redox conditions with a flow-through experiment. J. Nucl. Mater., 297, pp. 231-243.

Spahiu K., Eklund U.-B., Cui D. and Lundström M. (2002). The influence of near field redox conditions on spent fuel leaching. In: Scientific Basis for Nuclear Waste Management XXV, Mat. Res. Soc. Symp. Series, 713, pp. 633-638.

Spahiu K., Cui D. and Lundström M. (2004). The fate of radiolytic oxidants during spent fuel leaching in the presence of dissolved near field hydrogen. Radiochim. Acta, 92, pp. 625-629.